AGU PUBLICATIONS

Geophysical Research Letters

RESEARCH LETTER
10.1002/2014GL059335

Key Points:
- GIS compilation of potentially active continental low-angle normal faults
- Fifty percent chance of large earthquake in 35 years if all LANFs are seismically active
- No observed quakes moderately decreases likelihood that LANFs are seismogenic

Correspondence to:
R. H. Styron,
richard.h.styron@gmail.com

Citation:
Styron, R. H., and E. A. Hetland (2014), Estimated likelihood of observing a large earthquake on a continental low-angle normal fault and implications for low-angle normal fault activity, *Geophys. Res. Lett.*, *41*, 2342–2350, doi:10.1002/2014GL059335.

Received 17 JAN 2014
Accepted 19 MAR 2014
Accepted article online 21 MAR 2014
Published online 9 APR 2014

Estimated likelihood of observing a large earthquake on a continental low-angle normal fault and implications for low-angle normal fault activity

Richard H. Styron[1] and Eric A. Hetland[1]

[1]Department of Earth and Environmental Sciences, University of Michigan, Ann Arbor, Michigan, USA

Abstract The lack of observed continental earthquakes that clearly occurred on low-angle normal faults (LANFs) may indicate that these structures are not seismically active or that these earthquakes are simply rare events. To address this, we compile all potentially active continental LANFs (24 in total) and calculate the likelihood of observing a significant earthquake on them over periods of 1–100 years. This probability depends on several factors including the frequency-magnitude distribution. For either a characteristic or Gutenberg-Richter distribution, we calculate a probability of about 0.5 that an earthquake greater than *M*6.5 (large enough to avoid ambiguity in dip angle) will be observed on any LANF in a period of 35 years, which is the current length of the global centroid moment tensor catalog. We then use Bayes' Theorem to illustrate how the absence of observed significant LANF seismicity over the catalog period moderately decreases the likelihood that the structures generate large earthquakes.

1. Introduction

Low-angle normal faults (LANFs), with dips less than 30°, are well described in the geologic record. They are thought to play an important role in accommodating large-magnitude continental extension [*Howard and John*, 1987] and crustal thinning [*Lister et al.*, 1986], and their recognition has been a major development in continental tectonics [*Wernicke*, 2009]. However, despite widespread field observations of inactive LANFs and their central role in extensional tectonic theory, they remain enigmatic and contentious structures, and it is not clear if they are seismically active at low dip angles in the upper crust. This is for two reasons: because brittle faulting on LANFs is in apparent conflict with standard Andersonian rock mechanical theory as typically applied to the upper crust [*Axen*, 2004] and because observations of active, seismic faulting on LANFs are sparse and at times ambiguous. A considerable amount of research has been performed to address the former concern, reconciling LANF slip with rock mechanics [e.g., *Axen and Bartley*, 1997; *Collettini*, 2011]. The latter issue is highlighted by studies that have searched the focal mechanism catalogs and found no normal faulting earthquakes with focal mechanisms and surface ruptures clearly indicating slip on planes $\leq 30°$ [*Jackson*, 1987; *Collettini and Sibson*, 2001], which is taken as conclusive evidence that LANFs are inactive or aseismic. However, as noted by *Wernicke* [1995], the lack of observed seismic slip on continental LANFs may be simply because they are structures with comparatively long recurrence intervals, so earthquakes on them are infrequent. Alternately, active LANFs may have typical recurrence intervals but may simply be rare structures. Without knowing the likelihood of observing an LANF rupture in a time window of a few decades, it is not clear if an empty search result is strong evidence against LANF seismicity. If this likelihood is known, though, Bayesian probability theory provides a framework for quantifying how the negative search results impact the probability that LANFs are seismogenic.

In this work, we estimate the maximum likelihood of a significant LANF event occurring in time windows from 1 to 100 years, and then we interpret the lack of observed LANF seismicity in a quantified, probabilistic context using Bayes' Theorem. We estimate the maximum observation likelihood by treating all potentially active LANFs described in the literature as seismically active at their surface dip angles throughout the upper crust. Under these assumptions, we create synthetic earthquake catalogs with both Gutenberg-Richter and "characteristic" frequency-magnitude distributions, using each fault's geometry and slip rate. We then calculate the probability of observing earthquakes on at least one LANF over different observation periods. Finally, we use Bayes' Theorem to incorporate the negative catalog search results

and the observance likelihood to show how the negative results reduce the probability that LANFs are seismically active but do not bring the final probability to zero.

1.1. LANF Slip, Mohr-Coulomb Failure Theory, and Earthquakes

Areas of the crust undergoing active extension are generally assumed to have a subvertical maximum compressive stress. Mohr-Coulomb theory, as applied to the crust, predicts that a fault with a typical coefficient of friction for rocks (0.6–0.8) should lock up if it is oriented at an angle greater than 60° to the maximum compressive stress (i.e., fault dips less than 30°), and new, optimally oriented faults should form [*Sibson*, 1985]. Therefore, slip on normal faults with dips less than 30° may require much lower fault friction, elevated pore fluid pressure, significant local reorientation of the stress field at depth [e.g., *Yin*, 1989; *Selverstone et al.*, 2012], and/or failure under transtensional stress conditions [*Axen and Selverstone*, 1994].

Seismic evidence for slip on LANFs is sparse. This is partly due to the ambiguity of the rupture plane in earthquake focal mechanisms, as a focal mechanism with a low-angle nodal plane will also by definition have a high-angle nodal plane. Without ancillary information indicating which nodal plane corresponds to the slip surface, searches of earthquake catalogs cannot yield unique results as to whether they contain LANF events. Several collections of normal fault earthquakes with known surface breaks [*Jackson*, 1987; *Collettini and Sibson*, 2001], thereby resolving dip ambiguity, contain no low-angle events, although we note the total number of events in these collections are small ($\leq$ 25 events). Some candidate LANF events exist, but they are undersea [e.g., *Abers*, 2001] or difficult to verify [e.g., *Doser*, 1987]. In other cases, microseismicity in active rifts outlines low-angle detachment faults [e.g., *Monigle et al.*, 2012], but this does not necessarily mean these detachments rupture in large earthquakes.

Geologic evidence for LANF slip is more plentiful. Many potentially active LANFs have well-defined fault scarps in Quaternary sediments [e.g., *Styron et al.*, 2013; *Kapp et al.*, 2005; *Hayman et al.*, 2003; *Axen et al.*, 1999]. Some LANFs display pseudotachylytes [e.g., *Lister and Davis*, 1989], indicating seismic slip; a compelling example is found in the West Salton detachment, which gives strong evidence of seismic slip at low dip angles [*Prante et al.*, 2014].

In the Bayesian context of this study, evidence from geology, seismic profiling, Mohr-Coulomb failure theory, or any other information aside from earthquake focal mechanisms is considered to help construct the prior probability that LANFs rupture in large earthquakes. However, this study does not attempt to synthesize all available information and arrive at a single prior (or posterior) probability, to do so would necessarily involve making contentious decisions that could quickly become obsolete as evidence for or against LANF seismicity accumulates. Instead, this study illustrates how *any* prior probability may be quantitatively adjusted based on the likelihood of observing a significant LANF earthquake over some finite observation period and the fact that no such earthquakes have been definitively identified in the focal mechanism catalogs.

2. Potentially Active LANFs

Over the past decade or so, many field studies have found evidence for LANF activity in orogens throughout the world. These studies typically find arrays of Quaternary normal fault scarps on the fault traces and/or in the hanging walls of mapped or inferred low-angle detachment faults [e.g., *Axen et al.*, 1999]. Some studies also have bedrock thermochronology data from the exhumed detachment footwalls that are suggestive of ongoing rapid exhumation [e.g., *Sundell et al.*, 2013], although these data do not preclude a recent cessation of faulting. In some cases, additional evidence for LANF activity comes from geophysical data such as GPS geodesy [e.g., *Hreinsdóttir and Bennett*, 2009] and seismic waves [e.g., *Doser*, 1987].

We have compiled all potentially active LANFs with known subareal fault traces from a thorough review of the literature, finding 24 total (Figure 1). We have mapped the approximate fault traces into a geographic information system file (available at https://github.com/cossatot/LANF_gis), with metadata such as slip rate and source. Though the fault traces of many LANFs considered here are obscured by vegetation, others display large fault scarps in Quaternary sediments, particularly those in Tibet [e.g., *Styron et al.*, 2013; *Kapp et al.*, 2005] and western North America [e.g., *Axen et al.*, 1999; *Hayman et al.*, 2003], which are commonly interpreted as evidence for past seismic slip. About half are in Tibet, consistent with hypotheses that LANFs and metamorphic core complexes form in areas of hot, thick crust [e.g., *Buck*, 1991]. The rest are distributed through other areas of active continental extension: the North American Basin and Range, the Malay Archipelago, western Turkey, Italy, and Peru.

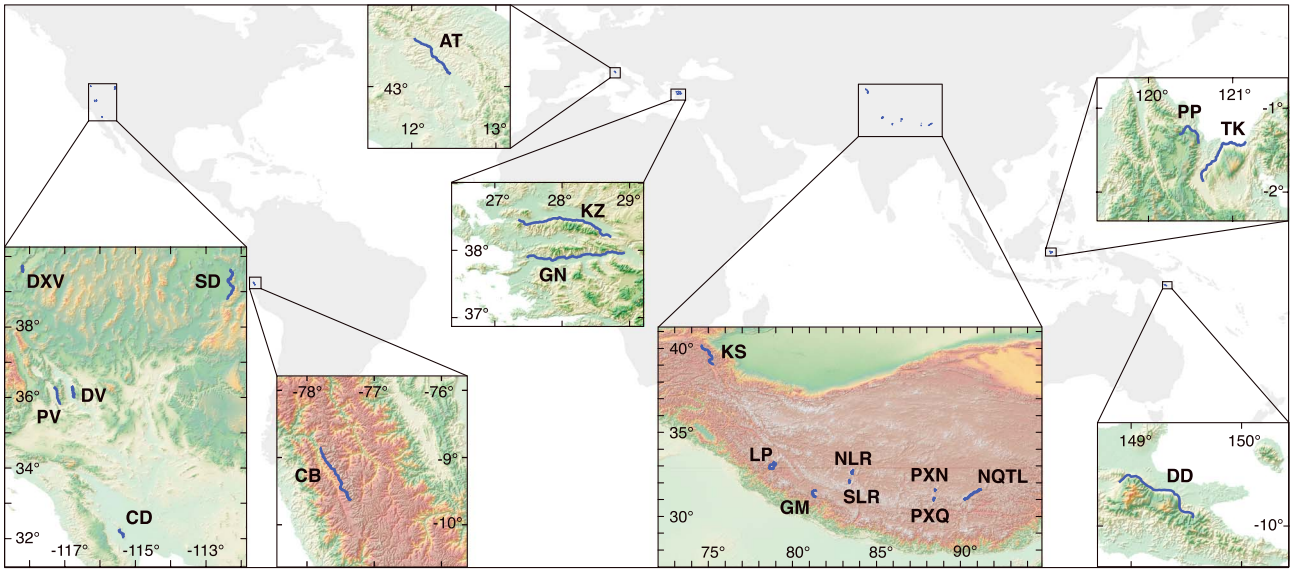

Figure 1. Map of known, potentially active continental LANFs (blue lines), with insets showing the physiographic context of the faults. DXV = Dixie Valley fault, PV = Panamint Valley fault, DV = Death Valley fault, CD = Cañada David detachment, SD = Sevier Desert detachment, CB = Cordillera Blanca detachment, AT = Alto Tiberina fault, KZ = Kuzey detachment, GN = Guney detachment, KS = Kongur Shan fault, LP = Leo Pargil detachment, GM = Gurla Mandhata detachment, NLR = North Lunggar detachment, SLR = South Lunggar detachment, PXN = Pum Qu–Xainza north fault, PXQ = Pum Qu–Xainza Qingdu fault, NQTL = Nyainqentanglha detachment, PP = Pompangeo detachment, TK = Tokorondo detachment, and DD = Dayman Dome.

Several of the most commonly cited candidates for seismically active LANFs were not included because they do not have a clearly defined, mappable fault trace, which is necessary for our earthquake likelihood calculations. These include the 1995 Aigion, Greece earthquake fault [*Bernard et al.*, 1997] and other potential LANFs underneath the Gulf of Corinth, and the 1952 Ancash, Peru earthquake fault [*Doser*, 1987]. Though submarine core complexes with superficially low angle detachments are well described in the literature and some of these structures may have produced recent earthquakes [*Abers*, 2001], we do not include these in our calculations for several reasons: (a) because mid-ocean ridges have not been structurally mapped with the completeness or resolution of subareal extensional provinces, it is not currently possible to come up with a reasonably complete inventory of ocean LANFs and (b) without high-resolution structural mapping and geodesy of oceanic LANFs, it is not possible to determine which structures in a mid-ocean ridge segment are currently active (seismically or not), and it is difficult to confidently associate particular earthquakes with a specific fault, given the high spatial density of normal faults at mid-ocean ridges.

3. Likelihood of Observing an LANF Event

3.1. Earthquake Likelihood on Individual LANFs

Wernicke [1995] developed a model, the W95 model, for the relationship between relative earthquake frequency and dip angle for normal faults, based on theoretical scaling relationships between mean coseismic stress drop, mean coseismic fault slip, fault dimensions, and far-field horizontal extension rates. W95 predicts that low-angle faults should rupture much less frequently than high-angle faults but in much larger earthquakes. We choose not to base our analysis on W95, as observations over the intervening two decades have shown that some of the necessary assumptions in the W95 model may be untenable. W95 is reliant upon proportional scaling relationships in which the constant of proportionality is unknown. The theoretical scaling between stress drop, fault dimensions, and slip used by W95 has been demonstrated to hold only at the order of magnitude level [*Leonard*, 2010], which is too coarse for our study. W95 also assumes that the fault strike length and downdip distance are approximately equal and therefore a function of dip and seismogenic thickness, which is not supported by the data in the LANF catalog we compiled, in which dip and strike length are uncorrelated. Finally, fixed velocity boundary conditions as assumed by W95 may be appropriate in regions of back-arc extension due to slab rollback, for example, but are not were extension occurs in response to elevated vertical stress from overthickened crust or gravitational potential excess, such as in western North America [*Jones et al.*, 1996], the Andes [*Dalmayrac and Molnar*, 1981], and Tibet [*Harrison et al.*, 1992], where the majority of active LANFs are found (Figure 1).

We estimate the likelihood of observing a significant earthquake on an individual LANF over some contiguous time window of length t years (up to 100) based on the estimated slip rate and fault geometry of each LANF. Because four of the LANFs are estimated to have slip rates less than 0.2 mm a^{-1} [*U.S. Geological Survey*, 2006] and therefore should have an extremely long recurrence interval for large earthquakes, we do not include these in the calculations. We perform a Monte Carlo simulation in which we create 4000 synthetic time series of earthquakes, with unique values for fault geometry and slip rate for each time series, sampled from the estimated values and uncertainties of each parameter. Then, for each time series we calculate the fraction of unique time windows of length t in which an earthquake as large or larger than a given magnitude occurs. We take this value as the probability of observing an earthquake greater than or equal to moment magnitude M over time period t, which we will refer to, in general, as $P(M, t)$. All calculations are performed with Python (v.2.7.5), using the Numpy [*Oliphant*, 2007], IPython [*Pérez and Granger*, 2007], Pandas [*McKinney*, 2010], and Joblib Parallel [*Varoquaux and Grisel*, 2009] packages. All codes and data for this project are available at https://github.com/cossatot/lanf_earthquake_likelihood/.

The geometry for each fault is estimated based on the length of the fault trace, the dip of the fault, and the estimated fault-locking depth in the area. The fault is treated as planar for simplicity of calculations. Even though the exposed footwalls of many detachment faults are nonplanar, ample geologic and geophysical evidence exists for listric [e.g., *Morley*, 2009], antilistric [e.g., *Styron et al.*, 2013; *Fletcher and Spelz*, 2009], and planar [e.g., *McGrew*, 1993] detachment geometries at depth; therefore, we consider treating the fault planes as planar to be the simplest treatment that is unlikely to systematically bias dip estimates at depth. We determine the fault length by measuring the approximate length of the mapped fault trace perpendicular to the assumed extension direction; for faults that change dip significantly along strike, we only consider the low-angle segments of the fault. Values for the dip are taken from the literature in most cases and measurements of the dip of footwall triangular facets (interpreted as the exhumed fault plane) from Shuttle Radar Topography Mission data otherwise. In all cases, ranges of fault geometries are considered, encompassing the degree to which the values are known. The fault-locking depth is assumed to be 10 km in the absence of other evidence (such as a geodetic study [e.g., *Hreinsdóttir and Bennett*, 2009]).

Slip rates of the 20 LANFs are gathered from the literature if possible or given broad ranges if not (e.g., 1–10 mm yr^{-1}). In the Monte Carlo simulation, samples for slip rate and dip are drawn from uniform distributions defined by the maximum and minimum values. Based on field observations, some faults have dip ranges that go above 30°, although for these fault dip values are sampled from the minimum to 30°, as here we only consider slip on faults shallower than 30°. The resulting probabilities on these faults are then multiplied by the fraction of the dip range that is $\leq 30°$.

Each synthetic earthquake sequence is generated by randomly sampling either 50,000 events from a tapered Gutenberg-Richter (GR) distribution with corner magnitude $M_c = 7.64$ and $\beta = 0.65$ (from values estimated by *Bird and Kagan* [2004] for continental rifts) or a 25,000 events from characteristic distribution. It is not certain which distribution more appropriately describes seismicity on a single LANF, though studies of many individual fault rupture histories suggest that the characteristic distribution is more accurate [e.g., *Hecker et al.*, 2013]. The smaller number of samples drawn from the characteristic distribution is due to the increased computation time associated with a higher proportion of large events, leading to much longer time series for a given number of events. The samples are taken from an interval $M = [5.0, M_{max}]$, where M_{max} is the moment magnitude associated with 15 m of slip over the given fault plane. We use the standard relations between fault slip, D, and moment magnitude, M, given by

$$M_o = \mu L z D / \sin \delta \tag{1}$$

and

$$M = 2/3 \log_{10}(M_o) - 6 \tag{2}$$

where L is the fault length, z is the seismogenic thickness, δ is the fault dip, $\mu = 30$ GPa is the shear modulus, and M_o is the seismic moment in N m [e.g., *Aki and Richards*, 2002; *Kagan*, 2003]. The characteristic distribution has a large-magnitude mode corresponding to $D = 1.5$ m on the fault, a typical slip distance for normal fault events [e.g., *Wesnousky*, 2008]. The distributions are shown in Figure 2.

These calculations rely on two important assumptions that warrant some discussion. The first is that each earthquake ruptures the entire fault patch uniformly. Though this is unlikely fault behavior, the long-term

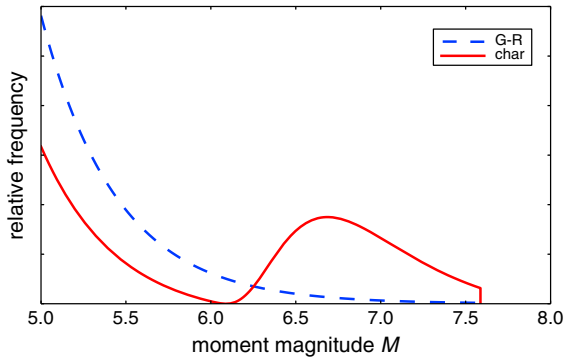

Figure 2. Gutenberg-Richter and characteristic frequency-magnitude distributions for the South Lunggar detachment.

statistical distribution of earthquake recurrence is insensitive to assumptions about slip distribution in individual events as long as earthquakes are unclustered in time (the second assumption discussed below). Specifically, if n different, equal fault patches rupture independently, each requires n times the interseismic strain accumulation time to rupture with an earthquake of magnitude M compared to the accumulation time for a single fault rupturing uniformly with much lower coseismic slip in each earthquake. Thus, magnitude M events would happen with the same long-term frequency. The next assumption is that earthquakes are ordered randomly and separated by the time necessary for sufficient strain to accumulate for each earthquake to occur. This means that foreshock and aftershock sequences and other types of event clustering are not taken into account. However, the modal interevent times for earthquakes $\geq M6$ or so are greater than a hundred years for most LANFs, so the ordering of events does not impact the results, as this is longer than our maximum observation window. Furthermore, any clustering resulting in event spacing less than the observation window would decrease $P(M, t)$, and here we choose to calculate the maximum $P(M, t)$ using the simplest assumptions, rather than choose the model assumptions such that the calculated probabilities are the minimum.

The results for faults with a GR frequency-magnitude distribution indicate that it is unlikely that any individual fault would have an earthquake greater than M 5 in any observation time window up to 100 years. As an example, the results for the Panamint Valley fault are shown in Figure 3a; this fault has the highest $P(M, t)$ of any of the well-studied LANFs. The probability of observing a $\geq$ M 6.0 event on the Panamint Valley fault is about 0.5 for t = 100 years and about 0.15 for t = 35 years, which is the current length of the global CMT catalog. As expected, given the GR distribution, $P(M, t)$ is much higher for smaller, more frequent events than for larger events. The modal recurrence intervals for $M \geq 6.5$ events are in the hundreds of years for 17 of the 20 faults studied; the longer of these are on the Pumxu–Xainza rift (Tibet) and Dixie Valley fault (Nevada, USA), which all have very short fault traces (10–20 km) and low slip rates ($\leq$ 1 mm a^{-1}).

The results for faults with a characteristic frequency-magnitude distribution yield much lower $P(M, t)$ for small to moderate events, but $P(M, t)$ is higher for large events(Figures 3b and 3d); this is because the earthquake sequences are dominated by large, infrequent events, so the interevent times for moderate events are several times greater. For the Panamint Valley fault, $P(M \geq 5, t = 35)$ is about 0.07 (versus 0.25 for the GR distribution), but $P(M \geq 7, t = 35)$ is around 0.025 (versus essentially zero for the GR distribution). As the characteristic distribution likely better represents earthquakes on an individual large fault, these results suggest that it is very unlikely that we would expect to capture any significant seismicity on an single LANF in the focal mechanism catalogs. The modal recurrence intervals for $M \geq 6.5$ earthquakes are, in general, shorter than for the GR distribution, as more strain release occurs during large events. These recurrence intervals are shorter than typical normal fault recurrence intervals but consistent with faults in rapidly deforming regions such as the Aegean and New Zealand [*Nicol et al.*, 2005]; however, these recurrence intervals are much shorter than the model of *Wernicke* [1995], in which it is argued that LANFs have an order of magnitude longer recurrence intervals than steeper normal faults.

3.2. Earthquake Likelihood on All LANFs

To calculate the probability of observing at least one earthquake on any of these LANFs during a given time period, we first assume that seismicity on each fault is independent and uncorrelated with seismicity on all other faults. This assumption is likely true for most faults. It may not be true for the few proximal faults, though it is unclear how these faults may interact such that an appropriate joint probability may be calculated. We determine the probability for each time window and minimum magnitude with the equation

$$P_{\text{AT or LP or } \ldots \text{ or DV}} = 1 - (Q_{\text{AT}} \cdot Q_{\text{LP}} \cdot \ldots \cdot Q_{\text{DV}}) \quad (3)$$

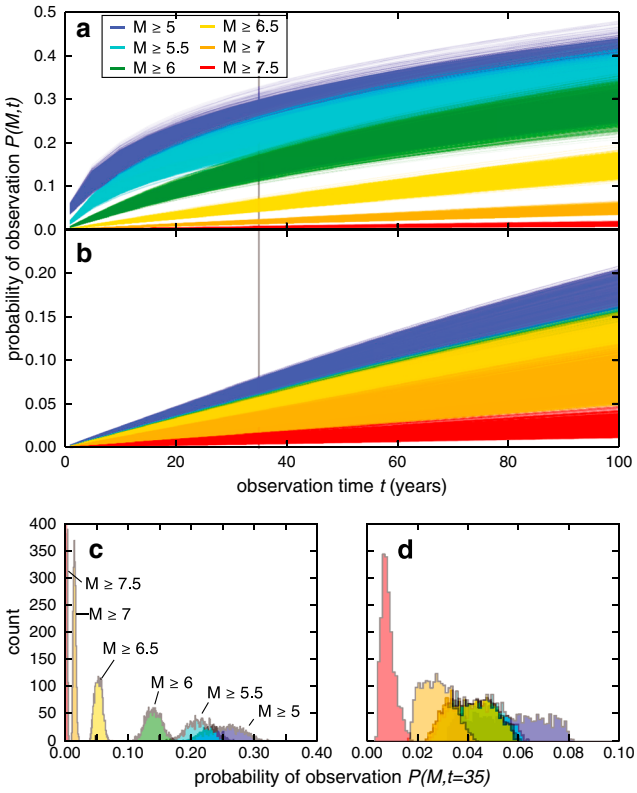

Figure 3. Probabilities of observing an earthquake greater than or equal to a given moment magnitude M over a given observation window on the Panamint Valley fault for (a) the Gutenberg-Richter distribution and (b) the characteristic distribution. Note the change in the scale of the y axis. (c) Cross section through Figure 3a at $t = 35$ years, showing the distributions of $P(M)$. (d) Cross section through Figure 3b at $t = 35$ years, showing the distributions of $P(M)$.

where P_{AT} is the probability of observing an earthquake on a single LANF (e.g., the Alto Tiberina fault) and $Q_{AT} = 1 - P_{AT}$. Equation (3) is the union of probabilities for nonmutually exclusive random events.

The results of this calculation are shown in Figures 4a and 4b. For the Gutenberg-Richter distribution, the likelihood of observing an LANF earthquake on any fault over a given observation period is quite high. For example, $P(M, t)$ for $M \geq 6$ and $t = 35$ years is about 0.85 and for the smaller events is quite close to 1. This high likelihood suggests that given the model assumptions, we should expect to find such an earthquake in the focal mechanism catalogs, although because many $M6$ events are not surface breaking [*Hecker et al.*, 2013], it might be difficult to unambiguously determine whether the high- or low-angle nodal plane slipped. For $M \geq 6.5$, the probability of observing an LANF earthquake is about 0.5, and the nodal plane ambiguity should be much less (e.g., due to surface scarps or directivity effects). The results for the characteristic distribution are lower than the results for the GR distribution for smaller events and higher for larger events, similar to the patterns seen in results for individual faults. $P(M \geq 5.5, t = 35)$ through $P(M \geq 6.5, t = 35)$ are all close, about 0.4–0.5.

3.3. Bayesian Adjustments of LANF Earthquake Likelihood

Because the earthquake focal mechanism catalog is much shorter than the repeat time for moderate to large earthquakes on typical normal faults with mm yr^{-1} slip rates, catalog searches yielding no results for a particular class of events cannot be definitive evidence that they do not occur. Nevertheless, the absence of observations does provide some evidence against their existence. Through Bayes' Theorem, we can use the probability of observing an event (i.e., $P(M, t)$) to calculate the likelihood that LANFs are active given the negative outcome of catalog searches. In this manner, Bayes' Theorem gives an adjusted, posterior likelihood for a given prior likelihood that LANFs are capable of generating large earthquakes. Different priors may result from different evidence or assumptions and are not likely to be constant through time or among all researchers. We do not choose a specific prior for LANF activity; rather, we calculate the posteriors over the range of prior probabilities from 0 (meaning no probability that LANFs are seismically active) to 1 (meaning LANFs are absolutely seismically active). Here $P(A)$ represents the prior probability for LANF seismic activity, and $P(O)$ is the probability of a positive test result (observation of an LANF earthquake in a catalog search). The symbol "~" indicates *not*, so $P(\sim \mathrm{A})$ is the probability that LANFs are inactive; $P(\sim \mathrm{A}) = 1 - P(A)$. The results of this study give us the probability of observing or not observing an LANF event given LANF seismic activity $P(O|A)$ and $P(\sim O|A) = 1 - P(O|A)$, respectively. $P(O| \sim A)$ is the probability of observing a "false positive", the incorrect identification of an LANF event, when in fact LANFs are not active. The posterior $P(A| \sim O)$ is the likelihood that LANFs can generate large earthquakes given that no LANF events have been observed and through Bayes' Theorem

$$P(A| \sim O) = \frac{P(\sim O|A)P(A)}{P(\sim O|A)P(A) + P(\sim O| \sim A)P(\sim A)}. \quad (4)$$

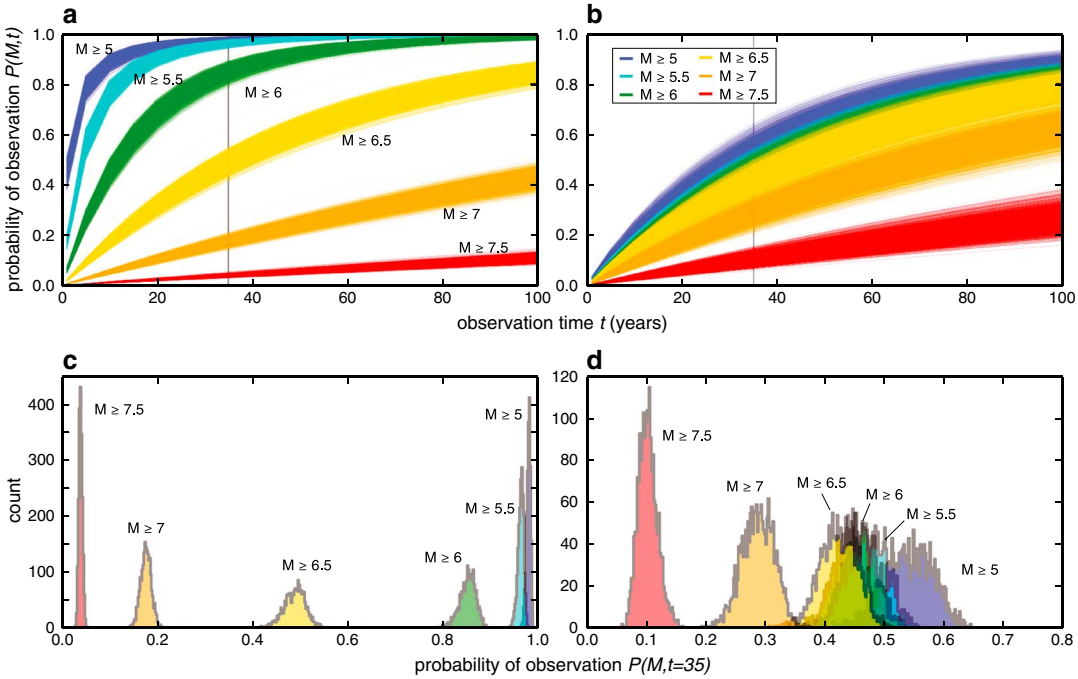

Figure 4. Probabilities of observing an earthquake greater than or equal to a given moment magnitude M over a given observation window on any LANF, given a (a) Gutenberg-Richter distribution and (b) a characteristic distribution. (c) Cross section through Figures 4a at t = 35 years showing probability distributions. (d) Cross section through Figures 4b at t = 35 years showing probability distributions.

Figure 5 shows $P(A| \sim O)$ for $P(A) \in [0, 1]$, using values for $P(O|A)$ of 0.1, 0.5, and 0.8 and a likelihood of false positives $P(O| \sim A) = 0.01$. The likelihood of LANF seismicity decreases appreciably given a moderate $P(O|A)$ but does not decrease to zero. Low values of $P(O|A)$ yield posteriors that are almost unchanged from the priors; in other words, the fact that no LANF events have occurred does not change the prior assumptions that LANF events are not expected to occur. Additionally, for strong priors with values very close to 0 or 1, the posteriors are much closer to the priors, which is to say that it takes much more evidence to change strongly held positions. For less strongly held prior assumptions, the posterior probability that the LANFs are active is reduced compared to what the prior assumptions are. For example, in the case of a prior of 0.5 (meaning that there is a 50% chance that LANFs can generate large earthquakes), if $P(O|A) = 0.1$, then the posterior likelihood for LANF seismicity drops to ≈ 0.48 (Figure 5). In this case, the fact that a catalog search results in no identified LANF earthquake is noninformative. If $P(O|A) = 0.5$, the posterior drops to ≈ 0.34, a moderate reduction. On the other hand, if $P(O|A) = 0.8$, the posterior is ≈ 0.17.

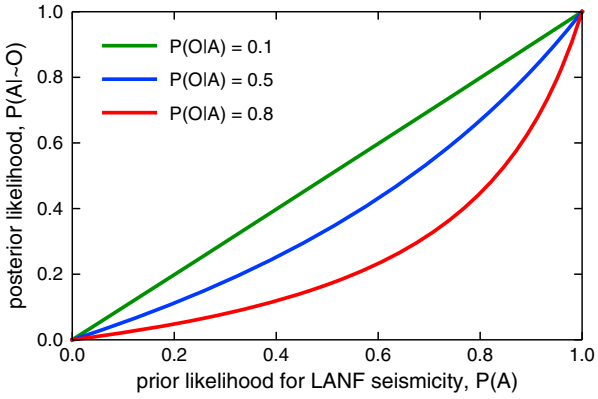

Figure 5. Prior likelihood for LANF seismicity $P(A)$ and posterior likelihood $P(A| \sim O)$ given no observed earthquakes. $P(O|A)$ is the likelihood of observing an earthquake given activity on all LANFs.

4. Discussion and Conclusions

Our compilation of all known potentially active LANFs shows that they are fairly uncommon structures, yet they still may be found in areas currently undergoing extension. Almost all major continental extensional regions are represented; notably, narrow, linear continental rifts, such as the East African and Rio Grande rifts, do not seem to contain active LANFs. This compilation may

serve as a point of comparison for different characteristics of active normal faults or LANF geometry or as a reference for any further study of these structures.

We regard our calculated $P(M, t)$ values as maximum estimates given our knowledge of existing active LANFs. As discussed above, part of the reason that $P(M, t)$ is the maximum is due to the fact that we assume declustered earthquake catalogs (Clustering on either a single fault or between proximal faults will decrease $P(M, t)$.). Additionally, $P(M, t)$ is a maximum estimate as we assume that all LANFs in this study are seismically active throughout the upper crust at surface dip angles. It is quite possible that some of these faults are not tectonically active at all. It is also possible that some or all of these detachments may be seismically active but at dip angles $\geq$ 30° at depth. For example, the Cañada David detachment in Mexico may dip very steeply at seismogenic depths [*Fletcher and Spelz*, 2009]. Some of these may also be aseismic; the Alto Tiberina fault appears to be creeping for much of its downdip extent [*Hreinsdóttir and Bennett*, 2009], and the neighboring Zuccale inactive LANF has fault gouge suggestive of creep [*Collettini and Holdsworth*, 2004]. If any individual fault is not seismically active at low angles, this reduces the total $P(M, t)$ for all events. On the other hand, it is quite unlikely that all candidate LANFs have been discovered, and we have not included several known candidates such as submarine detachments [e.g., *Abers*, 2001] or basal detachments without low-angle surface traces [e.g., *Bernard et al.*, 1997] because of the difficulty in quantifying their occurrence, geometry, and slip rates. Therefore, if the rate of inclusion of additional LANFs (due to discovery or further quantification of geometry and slip rate of poorly exposed LANFs) is higher than the rate of discreditation of LANFs considered here, then $P(M, t)$ values will increase. It should be noted, though, that the higher the $P(M, t)$, the more unlikely it becomes that LANFs slip in large earthquakes, as long as one has not been observed.

$P(M \geq 6.5, t = 35) \approx 0.5$ for either frequency-magnitude distribution and is a good reference value as events in this range are likely to be surface breaking, which would resolve the slip plane ambiguity inherent in earthquake focal mechanisms [*Hecker et al.*, 2013]. Given the fact that no significant LANF earthquakes have been definitively documented, this probability of an LANF earthquake occurring during a 35 year time window results in a lowering of any prior assumption that LANFs are active, as long as that prior assumption is not a strongly held position. The magnitude of the decrease depends on the prior likelihood, and the decrease is at most ~15% (from 0.5 to 0.35). This means that the current catalog length is much too short to be used as strong evidence against LANF seismicity. $P(M \geq 6.5, t = 100)$ is near 0.8 for both GR and characteristic distributions; this value more strongly reduces the likelihood of LANF seismicity yet still does not yield a definitive negative conclusion. Therefore, results of studies analyzing the dip distribution of earthquakes on continental normal faults [*Jackson*, 1987; *Collettini and Sibson*, 2001] should be interpreted as informative but not conclusive. Furthermore, alternative mechanisms for LANF slip such as aseismic creep [e.g., *Collettini*, 2011; *Hreinsdóttir and Bennett*, 2009], steep dips through most of the seimsogenic zone but shallower dips near the surface due to isostatic flexure [e.g., *Wernicke and Axen*, 1988], or relatively long seismic recurrence intervals [*Wernicke*, 1995] need not be invoked to explain the lack of observed seismicity, though these mechanisms may indeed be valid or well supported by other observations.

Acknowledgements
We thank Jon Spencer for a stimulating discussion that became the impetus for this study. Mike Taylor and Kurt Sundell provided valuable comments on a draft of the manuscript. Reviews by Gary Axen and Brian Wernicke were insightful and added clarity to the work.

The Editor thanks Brian Wernicke and Gary Axen for their assistance in evaluating this paper.

References

Abers, G. A. (2001), Evidence for seismogenic normal faults at shallow dips in continental rifts, *Geol. Soc. London Spec. Publ.*, *187*(1), 305–318.

Aki, K., and P. G. Richards (2002), *Quantitative Seismology: Theory and Methods*, University Science Books, Sausalito, Calif.

Axen, G. J. (2004), Mechanics of low-angle normal faults, in *Rheology and Deformation of the Lithosphere at Continental Margins*, edited by G. D. Karner et al., pp. 46–91, Columbia Univ. Press, New York.

Axen, G. J., and J. M. Bartley (1997), Field tests of rolling hinges: Existence, mechanical types, and implications for extensional tectonics, *J. Geophys. Res.*, *102*(B9), 20,515–20537.

Axen, G. J., and J. Selverstone (1994), Stress state and fluid-pressure level along the Whipple detachment fault, California, *Geology*, *22*(9), 835–838.

Axen, G. J., J. M. Fletcher, E. Cowgill, M. Murphy, P. Kapp, I. MacMillan, E. Ramos-Velázquez, and J. Aranda-Gómez (1999), Range-front fault scarps of the Sierra El Mayor, Baja California: Formed above an active low-angle normal fault?, *Geology*, *27*(3), 247–250.

Bernard, P., et al. (1997), The ms = 6.2, June 15, 1995 aigion earthquake (greece): Evidence for low angle normal faulting in the corinth rift, *J. Seismolog.*, *1*(2), 131–150.

Bird, P., and Y. Y. Kagan (2004), Plate-tectonic analysis of shallow seismicity: Apparent boundary width, beta, corner magnitude, coupled lithosphere thickness, and coupling in seven tectonic settings, *Bull. Seismol. Soc. Am.*, *94*(6), 2380–2399.

Buck, W. R. (1991), Modes of continental lithospheric extension, *J. Geophys. Res.*, *96*(B12), 20,161–20,178.

Collettini, C. (2011), The mechanical paradox of low-angle normal faults: Current understanding and open questions, *Tectonophysics*, *510*(3), 253–268.

Collettini, C., and R. Holdsworth (2004), Fault zone weakening and character of slip along low-angle normal faults: Insights from the Zuccale fault, Elba, Italy, *J. Geol. Soc.*, *161*(6), 1039–1051.
Collettini, C., and R. H. Sibson (2001), Normal faults, normal friction?, *Geology*, *29*(10), 927–930.
Dalmayrac, B., and P. Molnar (1981), Parallel thrust and normal faulting in Peru and constraints on the state of stress, *Earth Planet. Sci. Lett.*, *55*(3), 473–481.
Doser, D. I. (1987), The Ancash, Peru, earthquake of 1946 November 10: Evidence for low-angle normal faulting in the high Andes of northern Peru, *Geophys. J. R. Astron. Soc.*, *91*(1), 57–71.
Fletcher, J. M., and R. M. Spelz (2009), Patterns of Quaternary deformation and rupture propagation associated with an active low-angle normal fault, Laguna Salada, Mexico: Evidence of a rolling hinge?, *Geosphere*, *5*(4), 385–407.
Harrison, T. M., P. Copeland, W. Kidd, and A. Yin (1992), Raising Tibet, *Science*, *255*(5052), 1663–1670.
Hayman, N. W., J. R. Knott, D. S. Cowan, E. Nemser, and A. M. Sarna-Wojcicki (2003), Quaternary low-angle slip on detachment faults in Death Valley, California, *Geology*, *31*(4), 343–346.
Hecker, S., N. Abrahamson, and K. Wooddell (2013), Variability of displacement at a point: Implications for earthquake-size distribution and rupture hazard on faults, *Bull. Seismol. Soc. Am.*, *103*(2A), 651–674.
Howard, K. A., and B. E. John (1987), Crustal extension along a rooted system of imbricate low-angle faults: Colorado River extensional corridor, California and Arizona, *Geol. Soc. London Spec. Publ.*, *28*(1), 299–311.
Hreinsdóttir, S., and R. A. Bennett (2009), Active aseismic creep on the Alto Tiberina low-angle normal fault, Italy, *Geology*, *37*(8), 683–686.
Jackson, J. (1987), Active normal faulting and crustal extension, *Geol. Soc. London Spec. Publ.*, *28*(1), 3–17.
Jones, C. H., J. R. Unruh, and L. J. Sonder (1996), The role of gravitational potential energy in active deformation in the southwestern United States, *Nature*, *381*, 37–41.
Kagan, Y. Y. (2003), Accuracy of modern global earthquake catalogs, *Phys. Earth Planet. Inter.*, *135*(2), 173–209.
Kapp, J. L., T. M. Harrison, P. Kapp, M. Grove, O. M. Lovera, and D. Lin (2005), Nyainqentanglha Shan: A window into the tectonic, thermal, and geochemical evolution of the Lhasa block, southern Tibet, *J. Geophys. Res.*, *110*, B08413, doi:10.1029/2004JB003330.
Leonard, M. (2010), Earthquake fault scaling: Self-consistent relating of rupture length, width, average displacement, and moment release, *Bull. Seismol. Soc. Am.*, *100*(5A), 1971–1988.
Lister, G., M. Etheridge, and P. Symonds (1986), Detachment faulting and the evolution of passive continental margins, *Geology*, *14*(3), 246–250.
Lister, G. S., and G. A. Davis (1989), The origin of metamorphic core complexes and detachment faults formed during Tertiary continental extension in the northern Colorado River region, U.S.A., *J. Struct. Geol.*, *11*(1), 65–94.
McGrew, A. J. (1993), The origin and evolution of the southern Snake Range decollement, east central Nevada, *Tectonics*, *12*(1), 21–34.
McKinney, W. (2010), Data structures for statistical computing in Python, in *Proceedings of the 9th Python in Science Conference*, edited by S. van der Walt and J. Millman, pp. 51–56, SciPy, Austin, Tex.
Monigle, P. W., J. Nabelek, J. Braunmiller, and N. S. Carpenter (2012), Evidence for low-angle normal faulting in the Pumqu-Xianza Rift, Tibet, *Geophys. J. Int.*, *190*(3), 1335–1340.
Morley, C. K. (2009), Geometry and evolution of low-angle normal faults (LANF) within a Cenozoic high-angle rift system, Thailand: Implications for sedimentology and the mechanisms of LANF development, *Tectonics*, *28*(5), 1–30, doi:10.1029/2007TC002202.
Nicol, A., J. Walsh, T. Manzocchi, and N. Morewood (2005), Displacement rates and average earthquake recurrence intervals on normal faults, *J. Struct. Geol.*, *27*(3), 541–551.
Oliphant, T. E. (2007), Python for scientific computing, *Comput. Sci. Eng.*, *9*(3), 10–20.
Pérez, F., and B. E. Granger (2007), IPython: A system for interactive scientific computing, *Comput. Sci. Eng.*, *9*(3), 21–29.
Prante, M. R., J. P. Evans, S. U. Janecke, and A. Steely (2014), Evidence for paleoseismic slip on a continental low-angle normal fault: Tectonic pseudotachylyte from the West Salton detachment fault, CA, U.S.A., *Earth Planet. Sci. Lett.*, *387*, 170–183.
Selverstone, J., G. J. Axen, and A. Luther (2012), Fault localization controlled by fluid infiltration into mylonites: Formation and strength of low-angle normal faults in the midcrustal brittle-plastic transition, *J. Geophys. Res.*, *117*, B06210, doi:10.1029/2012JB009171.
Sibson, R. H. (1985), A note on fault reactivation, *J. Struct. Geol.*, *7*(6), 751–754.
Styron, R. H., M. H. Taylor, K. E. Sundell, D. F. Stockli, J. A. Oalmann, A. Möller, A. T. McCallister, D. Liu, and L. Ding (2013), Miocene initiation and acceleration of extension in the South Lunggar rift, western Tibet: Evolution of an active detachment system from structural mapping and (U-Th)/He thermochronology, *Tectonics*, *32*(4), 880–907, doi:10.1002/tect.20053.
Sundell, K. E., M. H. Taylor, R. H. Styron, D. F. Stockli, P. Kapp, C. Hager, D. Liu, and L. Ding (2013), Evidence for constriction and Pliocene acceleration of east-west extension in the North Lunggar rift region of west central Tibet, *Tectonics*, *32*(5), 1454–1479, doi:10.1002/tect.20086.
U.S. Geological Survey (2006), Quaternary fault and fold database for the United States. [Available at http://earthquake.usgs.gov/hazards/qfaults/.]
Varoquaux, G., and O. Grisel (2009), Joblib: Running Python function as pipeline jobs. [Available at https://pythonhosted.org/joblib/.]
Wernicke, B. (1995), Low-angle normal faults and seismicity: A review, *J. Geophys. Res.*, *100*(B10), 20,159–20,174.
Wernicke, B. (2009), The detachment era (1977–1982) and its role in revolutionizing continental tectonics, *Geol. Soc. London Spec. Publ.*, *321*(1), 1–8.
Wernicke, B., and G. J. Axen (1988), On the role of isostasy in the evolution of normal fault systems, *Geology*, *16*(9), 848–851.
Wesnousky, S. G. (2008), Displacement and geometrical characteristics of earthquake surface ruptures: Issues and implications for seismic-hazard analysis and the process of earthquake rupture, *Bull. Seismol. Soc. Am.*, *98*(4), 1609–1632, doi:10.1785/0120070111.
Yin, A. (1989), Origin of regional, rooted low-angle normal faults: A mechanical model and its tectonic implications, *Tectonics*, *8*(3), 469–482.